

Control of collective human behaviour: Social dynamics beyond modeling

Ilias Panagiotopoulos and Jens Starke*
*University of Rostock,
Institute of Mathematics,
18057 Rostock, Germany*

Wolfram Just
*Queen Mary University of London,
School of Mathematical Sciences, London,
E1 4NS, UK*
(Dated: November 2, 2022)

The motion of pedestrians is a paradigmatic phenomenon to study collective human behaviour. We propose a model-free approach to analyse the movement of pedestrians in experiments and get a quantitative understanding of crowd dynamics. Using concepts from control and analysis of dynamical systems we set up a scheme which allows us to identify dynamical unstable signatures in pedestrian flows. These signatures are the building blocks for crowd control and soft management of people, and thus result in a fundamental understanding of collective human behaviour. Our approach is entirely data driven and we provide a proof of concept by field and laboratory experiments. In addition, this methodology provides, based on experimental observations, quantitative benchmarks to judge the quality of mathematical models for pedestrian motion.

Keywords: non-invasive control, non-linear dynamics, bifurcation analysis of experiments, bi-stability, crowd control

I. INTRODUCTION AND CONTEXT

Modelling and control of collective human behaviour is one of the central themes of the 21st century, as for instance illustrated by crowd control issues at concerts or sport events or evacuation procedures for buildings. Most vividly these aspects are emphasized by extreme events such as the Hillsborough disaster [1], the Duisburg Love parade disaster [2] or the Kings Cross Station fire [3]. Studying and understanding pedestrian dynamics in a qualitative way may have a huge impact on crowds' safety (see e.g. [4–6]), individuals' comfort [7], infrastructures' design [8], and on implementing social distancing to prevent the spreading of diseases like Covid-19 [9–11].

There exist a large number of simulation programs [12–16] both based on computational fluid dynamics and discrete particle simulations impacting on governmental regulations and fire safety codes in many countries [17, 18]. In all these contexts theoretical modelling is in fact quite advanced and often in good agreement with actual data providing suitable input for a number of different standards for the design of critical infrastructure [19, 20]. However, they miss systematic experimental verification despite the work of a few experts (e.g. [21–27]), since setting up experiments in a socio technological context is a challenge.

Actual experiments in social systems pose a couple of substantial challenges. If we briefly adopt the notation predominantly used in statistics, social sciences, or medical clinical trials, experiments can be broadly

grouped in three different categories, namely statistical surveys where accurate average information about the behaviour of individuals can be obtained, observational studies which give detailed information about the dynamics of groups of people, and experimental studies where one impacts on a group of individuals and monitors the dynamical response. Such a classification is not sharp, the borders between the different categories are certainly blurred, and the classification may not fit perfectly in the physics context. Nevertheless, it helps to group the available experimental studies and to clarify our aim. For instance [28, 29] provide nice and very detailed overviews of properties of pedestrian motion obtained at an aggregate level. Experiments where one records the behaviour of groups of pedestrians subjected to static constraints and where one draws fundamental conclusions about the pedestrian flow are for instance the studies [30–32] giving among others detailed insight into the structure of the fundamental diagram, [33–35] which provide a comparison of actual experiments with models and discuss the identification of parameter choices, [26] which nicely illustrates state of the art technology to extract single trajectory information from experimental observations, or [36] which discusses in detail experimental observations to uncover the impact of diversity on the behaviour of crowds. Our approach follows the third paradigm where we aim to investigate the impact of small time dependent external inputs on the dynamics of a crowd. Thus, we broadly follow the concepts of response theory or spectroscopy developed e.g. in the context of condensed matter physics (see also [23]). In more detail, we apply in an experimental setup control techniques to study and track instabilities and bifurcations, a concept which is a powerful tool for the numerical investigation of nonlinear

* jens.starke@uni-rostock.de

76 model equations. A direct analysis of pedestrian experi-
 77 ments which uncovers changes of the qualitative dynam-
 78 ical behaviour, i.e. an experimental bifurcation analysis
 79 is lacking so far.

80 For our pedestrian experiments a sufficiently large
 81 number of individuals is crucial. Initial experimental tri-
 82 als with periodic boundary conditions where pedestrians
 83 entered a corridor repeatedly failed due to individuals
 84 memorizing their previous actions, adjusting their be-
 85 haviour, and substantially changing the dynamics of the
 86 crowd. As a result humans in our control experiments
 87 were allowed to participate in the experiment only once.
 88 Mass events like football matches or concerts provide
 89 many pedestrians when arriving at the location. How-
 90 ever, accompanying habits like pre-drinking alcohol cre-
 91 ates difficult non reproducible circumstances for experi-
 92 ments. Several trials failed as people disturbed deliber-
 93 ately the measurement processes. Reasonable conditions
 94 without hiring a large crowd can be found for example
 95 at public transport hubs during rush hours. We were
 96 unable to obtain permission to conduct experiments at
 97 bigger stations in Germany (Berlin and Hamburg) or in
 98 the UK (London), see e.g. [37] for the challenges one faces
 99 when one performs large scale pedestrian experiments in
 100 the public transport sector. We finally chose to perform
 101 experiments at the Ulmen-campus of the University of
 102 Rostock with first-semester students just starting their
 103 studies, and field experiments at the pier at Warnemünde
 104 port, where passengers are disembarking cruise ships.

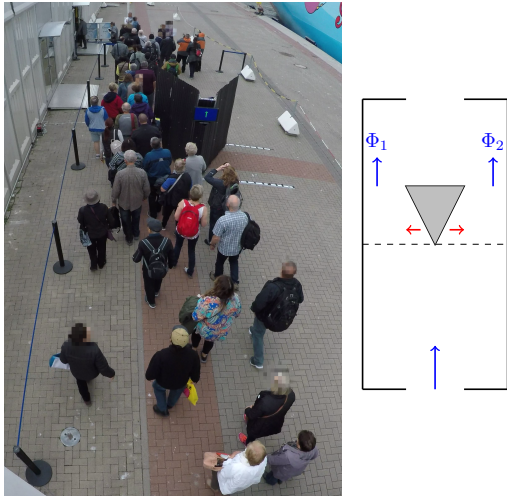


FIG. 1. Left: Route choice experiment of a pedestrian flow passing an obstacle. Right: Schematic setup of the experiment with corridor, obstacle and pedestrian flows indicated. The crucial parameter is the position of the obstacle and the relevant observable is given by the flux difference $\varphi = \Phi_1 - \Phi_2$ of pedestrians passing on the left and on the right of the obstacle.

105 As for the actual investigation, we analyse the route
 106 choice of individuals belonging to a crowd of people with
 107 the same target. This, for instance, could be a situation
 108 where people need to quickly move from one train plat-

109 form to another or where people have to choose a route
 110 to the exit of a building. To model such situations in a
 111 well-defined setup we design experiments where individ-
 112 uals aim to reach an exit at the end of a corridor (see Fig.
 113 1). A few meters in front of the exit a triangular obstacle
 114 blocks the pedestrians' direct way to the exit and gives
 115 them the option to manoeuvre around the right or left
 116 side of it. The pedestrian flux difference between passing
 117 left or right of the obstacle is the key quantity to be stud-
 118 ied, since this basic quantity gives us information about
 119 the route choice of the pedestrians and the crowding in
 120 the corridor. Of particular interest will be the effect of
 121 the obstacle's position on the flux difference.

122 The novelty of the current study comes in three parts.
 123 Firstly, by varying the position of the obstacle, we suc-
 124 ceeded in observing bistable states of the flow of human
 125 crowds. As a consequence, our findings indicate that in
 126 addition to stable flow patterns observed in experiments
 127 there are also unobservable, that means unstable, states
 128 which are crucial for understanding the overall global dy-
 129 namics. Secondly, we successfully applied an adaptive
 130 feedback controller to stabilise and reveal such unsta-
 131 ble states. Finally, we demonstrate how the features of
 132 pedestrian flows can be exploited to implement soft man-
 133 agement strategies [38], to achieve crowd control and to
 134 minimise crowding. By this, we mean measures which
 135 are indicative and provide guidance, such as signing [39].

136 The impact of our approach is twofold. On the one
 137 hand, we are able to propose suitable management and
 138 design strategies which minimise crowding and optimise
 139 social distancing. On the other hand, our approach can
 140 be used as an analytic tool to gain a better understand-
 141 ing of the dynamics of pedestrians. While our setup is
 142 quite basic, it turns out that the experiment we propose
 143 shares many features of real life pedestrian flows. We
 144 think our demonstration of successful soft management
 145 control strategies has considerable implications for real
 146 life human behaviour.

147 II. HYSTERESIS IN PEDESTRIAN FLOWS

148 We performed our study at two events with different
 149 focus. In the first set of experiments we aimed at a
 150 well defined and reproducible setup using a crowd with
 151 lower density, with less interpersonal relationships be-
 152 tween pedestrians and with a well defined pedestrian
 153 inflow. Hence we were emulating situations which are
 154 found in lab experiments in physics or chemistry with a
 155 well defined and reproducible environment. This series
 156 of experiments was conducted with first year students at
 157 the beginning of the autumn term at the University of
 158 Rostock. The key dynamical findings in this setup, i.e.,
 159 bistability and hysteresis of the pedestrian flow was then
 160 tested in a real world setup to ensure that our findings
 161 are not triggered by artefacts of lab setups. The second
 162 type of studies was performed on a pier in Warnemünde
 163 port where a crowd of people had just disembarked from

164 a cruise ship.

165 In both experiments people had to enter and exit a
 166 rectangular corridor designated by queue barriers. There
 167 was a single entrance and a single exit where all partici-
 168 pants were aiming for, see Fig. 1. A triangular obstacle
 169 was placed in the pedestrian's way to this single exit.
 170 The pedestrians passing the obstacle on either side were
 171 counted where, for the following of this paper, the left
 172 and right side is described from the pedestrians' point of
 173 view. The obstacle had a shape of an isosceles triangle,
 174 with the two sides being 2.2 m long and the third one
 175 being 1.8 m. The height of the obstacle was 2.4 m.

176 In the experiment conducted at Ulmencampus (see Fig.
 177 2 and blurred video at the Supplementary Material [40])
 178 our designated corridor was placed in front of the en-
 179 trance of a lecture theatre. The dimensions of the cor-
 180 ridor were 14 m long and 6 m wide. The width of the
 181 entrance and the exit was 1.2 m. There was an obstacle
 182 on the pedestrians' way, 6 m after the entrance (see Fig.
 183 1). Students wanted to enter the lecture theatre and were
 184 asked to wait shortly at the entrance of the corridor, so
 185 that a constant inflow rate at about 0.6 persons/s could
 186 be realised. In total, about 600 students participated. In
 187 the Warnemünde port experiment the dimensions of the
 188 corridor was 16 m long and 6 m wide, while the width
 189 of the entrance and the exit was 5 m. The obstacle was
 190 placed 8 m after the entrance. Over 1000 pedestrians
 191 participated, with an average inflow rate of around 1.5
 192 persons/s. Participants were people of different age and
 193 with no knowledge of the infrastructure but with the de-
 194 sire to reach quickly their target destination. During the
 195 experiments, we systematically moved the obstacle to dif-
 196 ferent positions and recorded the corresponding value of
 197 the flux difference φ_t . The process of moving the ob-
 198 stacle slowly was barely noticeable by the pedestrians,
 199 that means, in both cases, we perform a quasi-stationary
 200 parameter change, i.e., after each small increment we al-
 201 low the system to relax to a stationary state before we
 202 measure the current.

203 The variable of interest is a time-dependent flux differ-
 204 ence φ_t , that means the choice people make passing left
 205 or right of the obstacle. To measure this, we define φ_t
 206 to be the mean of the last 8 pedestrians' choice with +1
 207 for each one choosing the left side and -1 for the right
 208 side. We use the convention to assign positive values to
 209 people choosing the left side of the obstacle, $p_t = 1$, and
 210 negative values to the other side, $p_t = -1$, where t labels
 211 the time. Since the counter p_t is a strongly fluctuating
 212 quantity, in particular in cases with low density pedes-
 213 trian flows, we take an average of the last 8 pedestrians'
 214 crossings, $\varphi_t = 1/8 \cdot (p_t + p_{t-1} + \dots + p_{t-7})$, to measure the
 215 route choice difference. The window size of 8 results in
 216 a discrete measure φ_t which can take 9 different values
 217 with resolution ± 0.25 . This quantity provides enough
 218 information for our data-based and model-free approach.
 219 Most importantly no advanced tools for measuring the
 220 speed or the distances between pedestrians were needed.
 221 The results from the experiment at the Ulmencampus

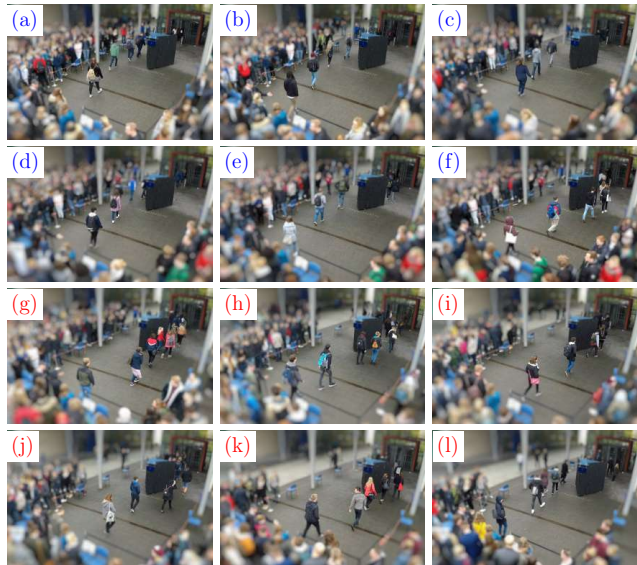
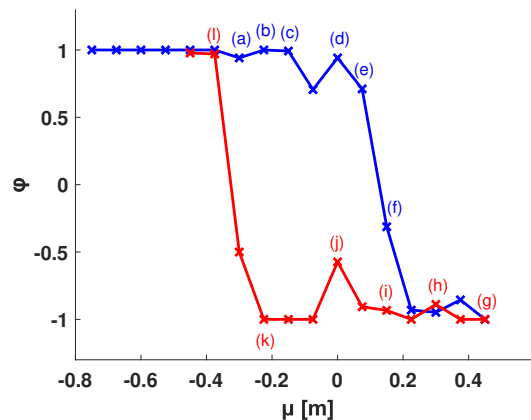


FIG. 2. Route choice experiment at Ulmencampus, University of Rostock. Top: measured mean flux difference as a function of the obstacle position, for up- (blue) and downsweep (red) of the system parameter showing hysteresis. Bottom: snapshots of the actual pedestrian configurations for different values of the obstacle position (see labels).

222 are presented in Fig. 2. With $\mu = 0$ denoting the center
 223 of the corridor, the obstacle was moved from negative
 224 to positive positions by small increments of 0.075 m and
 225 then back toward its initial positions. For each obstacle
 226 position, we allowed the flow to attain a new station-
 227 ary state before we moved the obstacle again. During
 228 this procedure, we observed a sudden change in peo-
 229 ple's choice for two different positions of the obstacle.
 230 This phenomenon is reflected by the mean flux differ-
 231 ence jumping from positive to negative values at around
 232 $\mu = 0.15$ m and then from negative to positive at about
 233 $\mu = -0.225$ m, see Fig. 2. The bottom part of Fig.
 234 2 shows the pedestrians' walking choice throughout the
 235 obstacle sweep. From the obstacle sweep, we observed
 236 that for any position $\mu \in [-0.225 \text{ m}, 0.15 \text{ m}]$ there are
 237 two different states of the system which seem to be sta-
 238 ble. When the obstacle position is changed, the choice

239 of the pedestrians depends on the previous state, which
 240 leads to a hysteresis phenomenon.

241 The results of the second series of experiment are
 242 shown in Fig. 3. Here passengers wanted to leave the pier
 243 at Warnemünde port. We had a quite diverse crowd at
 244 our disposal with individuals of a large range of ages and
 245 different nationalities, where pedestrians had no knowl-
 246 edge of the infrastructure they were about to cross. Pas-
 247 sengers did not just want to leave the pier as quickly
 248 as possible, but also to stay close to their friends and
 249 families. Unlike the first type of experiments, the sec-
 250 ond setup contained elements which broke the left-right
 251 symmetry. The dependence of the flux difference on the
 252 obstacle position is summarised in the top panel of Fig.
 253 3.

254 From the obstacle sweep, for any position $\mu \in$
 255 $[0.3 \text{ m}, 0.75 \text{ m}]$ there are two different states of the sys-
 256 tem which seem to be stable. The hysteresis is, however,
 257 not symmetric, as the interval of offsets μ for which we
 258 observe bistability is not centred around $\mu = 0$. There
 259 is a clear bias towards one side. Indeed, that was ex-
 260 pected since the Cruise Center was to the left and parallel
 261 to our designated corridor. Hence pedestrians favoured
 262 passing on the left side of the obstacle. Nevertheless,
 263 we still observed the previously recorded hysteresis phe-
 264 nomenon. In particular, our findings are robust under
 265 real world conditions, where, e.g., we do not monitor the
 266 inflow of pedestrians. Furthermore, hysteresis still per-
 267 sists under other inhomogeneities which occur frequently
 268 in social groups. For instance, we observed small groups
 269 of passengers, like families or friends, walking together or
 270 slowing down to wait for each other. We also observed
 271 moments where the density of pedestrians was higher or
 272 lower or even moments when there was a small gap in
 273 the flow. Neither of these imperfections had impact on
 274 the occurrence of the hysteresis phenomenon, which can
 275 hence be considered as a fairly robust property of a pedes-
 276 trian flow. Additionally, the phenomenon observed does
 277 not seem to be a cultural characteristic since the partic-
 278 ipants of the second series of experiment were tourists of
 279 different nationalities.

280 The results from both series of experiments indicate
 281 that for a range of positions of the obstacle two different
 282 states of the system coexist. The bistability observed in
 283 this system does not require a special type of geometric
 284 symmetry. It is robust against a bias, as illustrated in the
 285 results from the experiment at Warnemünde port. The
 286 hysteresis phenomenon appears also in a setup where the
 287 discrete nature of the measured flux difference is notic-
 288 able. We conclude that the dynamical signature, the hys-
 289 teresis caused by the route choice is a stable phenomenon
 290 which does not just occur under laboratory conditions,
 291 but reflects real-life situations of pedestrian flows.

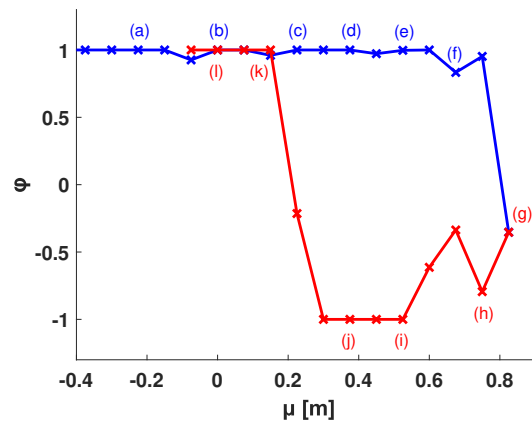


FIG. 3. Route choice experiment at the Warnemünde port. Top: measured mean flux difference as a function of the obstacle position, for up- (blue) and downsweep (red) showing hysteresis. Bottom: snapshots of the actual pedestrian configurations for different values of the obstacle position (see labels).

292 III. NON-INVASIVE CONTROL: SOFT 293 MANAGEMENT STRATEGIES

294 Crowd or traffic management [41–43] can be considered
 295 as a particularly challenging engineering control problem
 296 where one uses small control inputs for guiding people.
 297 Such soft strategies are actions, suggestions or guidelines
 298 that pedestrians could ignore like markings on the floor,
 299 signs, traffic indicators for different routes. Control with
 300 minimal invasion has been re-emphasised in science, in
 301 particular, in the context of controlling complex dynam-
 302 ical behaviour [44]. Feedback control exploits the dy-

303 nautical features of the underlying dynamics, making a
 304 large variety of potential target states accessible. In addition,
 305 control can also be used to explore the features of a
 306 system (see e.g. [45–50]) where one mimics within an ex-
 307 perimental setup continuation techniques used for bifur-
 308 cation analysis. Hence control in this context has a sec-
 309 ond facet, namely, employing the technique for the anal-
 310 ysis and spectroscopy of complex dynamical behaviour.
 311 Within our experimental setup we have the ideal testbed
 312 to study non-invasive control in a socio-dynamical con-
 313 text. The measurements presented in the previous sec-
 314 tion and the general theory of dynamical systems suggest
 315 that an additional, unstable and therefore unobservable
 316 state of the system exists in the bistability region. As we
 317 operate in the neighbourhood of a stationary state, con-
 318 trol is possible with minimal control forces. We aim to
 319 control an unknown unstable steady state with asymp-
 320 totically vanishing control force, while at the same time
 321 we have limited possibilities to act on our system. We
 322 employ here soft management strategies, i.e., by signs or
 323 traffic lights, as opposed to hard management strategies
 324 which are invasive like barriers or bouncers.

325 Controlling unknown states is quite well known in en-
 326 gineering and can be achieved by a state observer. As for
 327 the actual control algorithm we follow a suggestion of [51]
 328 which in fact is a simple realisation of feedback control
 329 with a state observer. To illustrate the basic idea recall
 330 that the flux difference measuring the pedestrians choice,
 331 φ_t , is the quantity of interest. Assume for the purpose
 332 of illustration that the time evolution can be approxi-
 333 mately captured by an unknown differential equation of
 334 the type $\dot{\varphi}_t = G(\varphi_t)$ with unstable stationary state φ_* ,
 335 which implies $G(\varphi_*) = 0$. Adding a control force results
 336 in $\dot{\varphi}_t = \tilde{G}(\varphi_t, a(y_t - \varphi_t)) = G(\varphi_t) + a(y_t - \varphi_t)$ with
 337 a being the gain of the control loop. We here consider
 338 the simple case that the dynamics of the control device
 339 is governed by a linear law $\dot{y}_t = b(y_t - \varphi_t)$ with filter
 340 parameter b . The dynamical state y_t of the controller es-
 341 timates the value of this unknown unstable state and can
 342 be considered as the simplest incarnation of a so called
 343 state observer. The control signal $y_t - \varphi_t$ is then fed back
 344 to our original dynamical system resulting in the closed
 345 loop dynamics $\dot{\varphi}_t = \tilde{G}(\varphi_t, a(y_t - \varphi_t))$ with a being the
 346 gain of the control loop. The fixed point of this closed
 347 loop dynamics is clearly given by $y_* = \varphi_*$ and $G(\varphi_*) = 0$,
 348 i.e., y_* estimates the unknown fixed point which coincides
 349 with a fixed point φ_* of the original equation of motion.
 350 Furthermore the feasibility of the control algorithm can
 351 be established by a simple linear stability analysis. If
 352 φ_* is an unstable fixed point with positive eigenvalue
 353 $G'(\varphi_*) > 0$, then linear stability analysis easily shows
 354 that stability of the closed loop dynamics with the state
 355 observer is achieved if $b > 0$ and $a > G'(\varphi_*) + b$. In
 356 particular, the actual control signal becomes small and
 357 asymptotically tends to zero, so that the approach works
 358 with tiny control forces. Implementation does not need
 359 any knowledge about the stationary state or the under-
 360 lying equations of motion. This, in practice, means that

361 the external force induced by signs is in principle able
 362 to drive the system to unobservable states, and it van-
 363 ishes when the system operates around an unstable fixed
 364 point.

365 The diagram Fig. 2 is the result of a fairly complex
 366 dynamical system with many degrees of freedom, but it
 367 resembles a structure which can also be seen in a low-
 368 dimensional effective equation of motion. Equation free
 369 analysis [52] aims at reducing the dynamics of a complex
 370 system, normally given in terms of a high-dimensional
 371 system of differential equations, to a low-dimensional ef-
 372 fective equation of motion just based on numerical sim-
 373 ulations. Here we take this idea a crucial step further
 374 [47, 48]. We explore, whether it is possible to use mea-
 375 surements and control techniques in our pedestrian flow
 376 to identify signatures of such a low-dimensional effective
 377 equation of motion. Using the analogy with bifurcation
 378 analysis the result shown in Fig. 2 suggests that there ex-
 379 ists an additional unstable branch of states. Such unsta-
 380 ble flow patterns correspond to an unstable fixed point in
 381 an effective low-dimensional description. Using the con-
 382 trol algorithm described above we aim to track unstable,
 383 i.e., unobservable states, in dependence of the obstacle
 384 position μ . Unlike in numerical simulations, where ini-
 385 tial conditions are at the disposal of the programmer, we
 386 have only very limited control, if at all, over the initial
 387 state of the system. In practice we just let pedestrians
 388 enter the corridor. We are however able to change the po-
 389 sition of the obstacle, μ , and we can set the initial state of
 390 the observer variable, $y_{t=0}$, which estimates the unknown
 391 effective fixed point and then dynamically adjusts to the
 392 true value of the originally unstable flux difference.

393 The experiments with control were conducted at the
 394 Ulmencampus with the same configuration as described
 395 in the previous section. To implement a soft management
 396 strategy we displayed an arrow on a monitor mounted at
 397 the obstacle but we didn't give any further incentive to
 398 the pedestrians to follow this sign. For the control scheme
 399 the arrow was inclined and magnified giving the pedes-
 400 trians an indication on which side to pass the obstacle.
 401 The inclination and size of the arrow was adjusted pro-
 402 portionally to the control signal $y_t - \varphi_t$, with positive
 403 or negative values corresponding to an arrow inclined to-
 404 wards the right or left, respectively. Successful control
 405 is indicated by the system fluctuating around a state or,
 406 equivalently, reaching a new steady state, with small con-
 407 trol signal $y_t - \varphi_t$.

408 As for the protocol of the experiment with control,
 409 the following steps were performed. First, we made a
 410 prediction for an unstable state. The choice of these ini-
 411 tial values was made based on the sweep diagram as de-
 412 picted in Fig. 2. Although the diagram is not perfectly
 413 symmetric, it looks that the tipping points are around
 414 $(\mu, \varphi) = (-0.3, -1)$ and $(\mu, \varphi) = (0.3, 1)$. As a result, we
 415 expected the unknown steady states to lie in the vicini-
 416 ty of the line connecting these two points. Based on
 417 the sweep diagram of Fig. 2 we initialized our experi-
 418 ment with $\mu = 0$. For the differential equation governing

419 the state observer $\dot{y}_t = b(y_t - \varphi_t)$ we chose $y_{t=0} = 0$
 420 and $b = 0.05$. The parameter a that scales the arrow
 421 accordingly was chosen to be $a = 6$. In contrast to a
 422 numerical experiment where a model for the system under
 423 investigation is available, the pedestrians' state could
 424 not be set at will. As a result, we had no way to initial-
 425 ize the pedestrian at a given state. Instead, pedestrians
 426 started entering the corridor, walking towards the end of
 427 it and being influenced by the arrows displayed at the
 428 front of the corridor. As explained above, reaching a
 429 new steady state is equivalent to the system fluctuating
 430 around a state with small control signal $y_t - \varphi_t$. When
 431 this happened, we recorded the value around which φ_t
 432 fluctuates as a new steady state. At this point, we were
 433 ready to move to the next parameter value. Pedestrians
 434 kept walking inside the corridor as we moved the obsta-
 435 cle to $\mu = 0.075\text{m}$ and initialized the differential equation
 436 governing the state observer with $y_{t=0} = 0.25$. As soon
 437 as the experiment for this position of obstacle was suc-
 438 cessful, we continued with two more cases $\mu = 0.15\text{m}$,
 439 $y_{t=0} = 0.5$ and $\mu = 0.225\text{m}$, $y_{t=0} = 0.75$.

441 The results of the experiment with control are sum-
 442 marised in Fig. 4. Students were asked to walk through
 443 the corridor only once, as the memory of people going
 444 through the corridor several times would potentially al-
 445 ter the results. We conducted the experiment for four
 446 different positions of the obstacle and we managed to
 447 reveal additional unstable states, see the green circles
 448 Fig. 4. The middle part of Fig. 4 shows time traces of the
 449 various relevant quantities. The state of the controller y_t
 450 (red) quickly approaches the flux difference of the unsta-
 451 ble state and thus estimates the unobservable state suc-
 452 cessfully. The flux difference φ_t (blue) approaches the
 453 same value but shows larger fluctuations. These fluctu-
 454 ations are caused by the intrinsic discrete nature of the
 455 measured flow φ_t , which comes in units of 0.25. Con-
 456 vergence is better visible when we smoothen the data by a
 457 Cesaro average defined as $c_t = \sum_{k=1}^t p_k/t$ (cyan). Finally
 458 we show as well the pedestrians' choice $p_t = \pm 1$ (pur-
 459 ple circles) which clearly demonstrates that the pedes-
 460 trian flow under control is channelled along both sides
 461 of the obstacle. Above all the control signal $y_t - \varphi_t$ be-
 462 comes small when successful control is achieved so that
 463 the states shown in Fig. 4 are unstable solutions of an
 464 underlying dynamical system.

465 In addition to the data obtained from this experiment,
 466 the top panel of Fig. 4 also contains the mean flux differ-
 467 ence observed in the experiment without control (cf. Fig.
 468 2). Some of the controlled states are almost outside the
 469 observed hysteresis region. The actual bistability region
 470 is certainly larger than recorded since noise, imperfec-
 471 tions, and finite size effects render some of the observ-
 472 able stable states unstable, a phenomenon which is preva-
 473 lent at the boundaries of the bistability region.

474 Unlike the uncontrolled pedestrian flow, the flow sub-
 475 jected to the control shows less crowding. A close in-
 476 spection of the controlled states reveals that the actual
 477 pedestrian flow is split into two parts with pedestrians

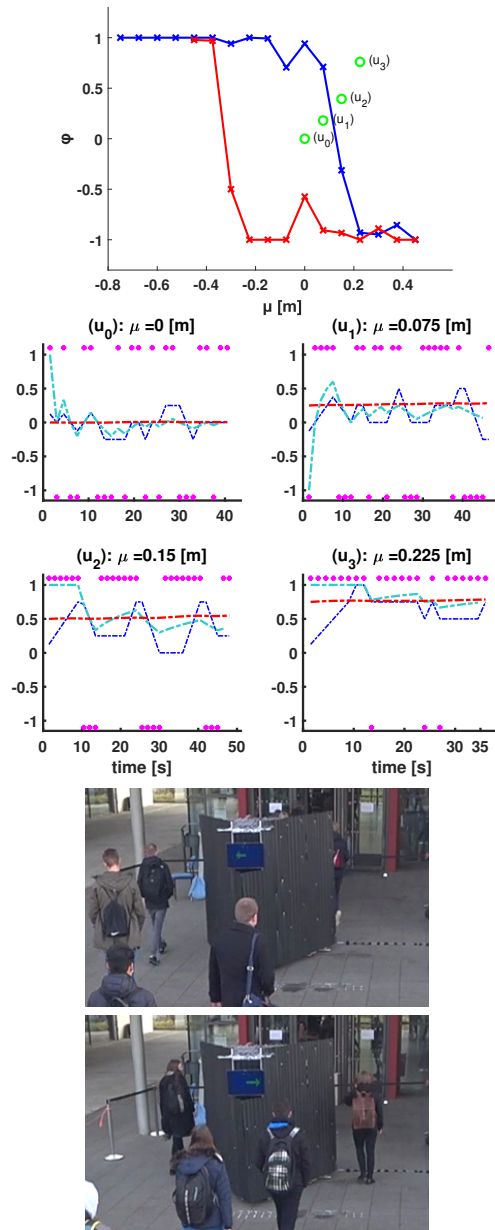


FIG. 4. Control of pedestrian flows at the Ulmencampus. Top: flux difference as a function of the obstacle position. Stabilised unstable states (green circles) for different positions of the obstacle; for comparison flux difference without control (see Fig. 2) for up- (blue) and down-sweep (red) of the parameter. Middle: the measured control flux difference φ_t as a function of time t (blue: actual flux difference, cyan: Cesaro average, see text for details), the state of the controller y_t which estimates the target state (red), and the time trace of the pedestrian count passing by the obstacle, i.e., p_t (purple circles). Bottom: snapshots of actual pedestrian configurations during control for $\mu = 0$. Control is implemented by the green arrow displayed on the screen.

478 passing by the obstacle on the left and on the right side
 479 (see e.g. purple circles in the middle part of Fig. 4 and the
 480 photos in the bottom part). Effectively the pedestrian

481 flow becomes less crowded and social distancing between
 482 pedestrians is enhanced. We achieved this by a minimally
 483 invasive control force which eventually becomes small. In
 484 addition, the optimal obstacle position for splitting the
 485 flow in the current symmetric set-up is certainly the po-
 486 sition without offset, $\mu = 0$, as the controlled flow differ-
 487 ence becomes minimal in this setup. While this feature
 488 is a consequence of the symmetries shared by our setup,
 489 the optimal obstacle position is less obvious in asymmet-
 490 ric situations (cf. Fig. 3).

491 In summary, we have implemented a soft management
 492 strategy where the control input becomes small when the
 493 target state is reached. We have achieved that success
 494 by exploiting the system dynamics. Our showcase proves
 495 that soft management strategies can give a better level
 496 of service if suitable unstable states in pedestrian flows
 497 can be identified, leading finally to a more efficient crowd
 498 management.

499 IV. MICROSCOPIC MODELS VS MODEL-FREE 500 APPROACH

501 The phenomena observed and described through the
 502 conducted experiments provide a good test for the vari-
 503 ous models of crowd behaviour, see e.g. [5, 53–55] for a
 504 review. One popular model which has been extensively
 505 used for pedestrian simulations is the *social force model*
 506 [56]. According to this model, pedestrians are described
 507 as particles and their motion is the result of social forces
 508 acting on them. These forces reflect the impact of their
 509 psychology and surroundings. The motion for pedestrian
 510 i is given by its acceleration

$$\ddot{\mathbf{x}}_i = \mathbf{F}_i + \sum_j \mathbf{f}_{ij} + \mathbf{f}_i^B, \quad (1)$$

511 where \mathbf{F}_i is the target force that drives an individual
 512 towards a specific target with a desired velocity, \mathbf{f}_{ij} are
 513 the interaction forces between pedestrians i and j and
 514 \mathbf{f}_i^B is the external repulsive force taking the effect of the
 515 walls and the obstacles into account. The target force is
 516 given by

$$\mathbf{F}_i = \frac{1}{\tau} (v_i \mathbf{e}_i - \dot{\mathbf{x}}), \quad (2)$$

517 where τ denotes the reaction time, v_i is the desired speed
 518 of pedestrian i and \mathbf{e}_i is their normalised target direction.
 519 The latter was adjusted to include the tendency to follow
 520 people around (see [57]). Specifically, the target direction
 521 of each pedestrian is a linear combination of the direction
 522 to the exit, \mathbf{e}_{\parallel} , and a weighted mean of the velocities $\langle \dot{\mathbf{x}}_j \rangle_i$
 523 over pedestrians j in a neighbourhood of pedestrian i

$$\mathbf{e}_i = \frac{(1 - \lambda) \mathbf{e}_{\parallel} + \lambda \langle \dot{\mathbf{x}}_j \rangle_i}{\|(1 - \lambda) \mathbf{e}_{\parallel} + \lambda \langle \dot{\mathbf{x}}_j \rangle_i\|}, \quad (3)$$

524 where λ denotes the *lemming parameter* which measures
 525 the psychological impact by pedestrians in the neighbour-
 526 hood. See [57, 58] for details.

527 Control by signage, traffic lights, or arrows is an in-
 528 herently complex process involving perception and psy-
 529 chology. Here we just map this complex process to an
 530 adjustment of the target direction. To implement the
 531 soft control strategy of our experiment (see Fig. 4), i.e.,
 532 to feed the control input to the model, we update the tar-
 533 get direction \mathbf{e}_i of pedestrians i . This results in a target
 534 direction with control

$$\mathbf{e}_i^c = \frac{\mathbf{e}_i + a(y - \varphi) \mathbf{n}_{\perp}}{\|\mathbf{e}_i + a(y - \varphi) \mathbf{n}_{\perp}\|}, \quad (4)$$

535 where \mathbf{n}_{\perp} denotes a vector perpendicular to the walls of
 536 the corridor. To take the local character of our experi-
 537 mental setup into account, which just relies on displaying
 538 arrows on the monitor in front of the obstacle, we update
 539 the control term \mathbf{e}_i^c only for pedestrians inside a small
 540 rectangular area in front of the obstacle visualised as a
 541 red box in the bottom part of Fig. 5. In order to verify
 542 this model we have performed a series of particle simu-
 543 lations similar to the experiments. The entire geometric
 544 configuration, e.g., corridor, obstacle and entrance were
 545 the same as in the experiment at Ulmencampus. We also
 546 ensured to always have 8 pedestrians inside the corridor.

547 For the numerical integration of the model, we take
 548 a lemming parameter $\lambda = 0.45$, a pedestrian-obstacle
 549 length scale of 1.5 m, a pedestrian-pedestrian repulsion
 550 parameter of $10 \text{ m}^2/\text{s}^{-2}$ and a pedestrian-pedestrian in-
 551 teraction range of 2 m. The control area was a rectangu-
 552 lar area of width 0.7 m and length 1.5 m placed (its closer
 553 side) 1.3 m in front of the obstacle. The control area was
 554 shifted together with the obstacle so that its center was
 555 always the tip of the triangular obstacle. The rest of the
 556 parameters of the simulation can be found in [57, 58].

557 While a microscopic numerical simulation allows for
 558 the application of the most subtle control algorithm we
 559 deliberately stayed with the protocol used in our experi-
 560 mental setup. We first emulated a parameter up- and
 561 downsweep to record the flux difference without control.
 562 In the second part of the numerical simulations we ap-
 563 plied the control scheme described above. Fig. 5 sum-
 564 marises our findings. In the top panel the blue and red
 565 lines correspond to the mean value of the measure φ with-
 566 out control for different position of the obstacle. Clearly,
 567 the experimental hysteresis phenomenon is reproduced
 568 even at a quantitative level (see Fig. 2). The green sym-
 569 bols show the states subjected to control. Again a re-
 570 markable quantitative agreement between the simulation
 571 results (circles) and experimental data (crosses) is found.
 572 The middle part of the figure shows the time series of the
 573 measure φ (blue line) and the controller variable y (red
 574 line) for four states of the system. The purple circles
 575 indicate the choice of each pedestrian. Even these mi-
 576 croscopic features of the simulations coincide remarkably
 577 well with the actual experimental time traces of Fig. 4.
 578 Similar to the results from the experiment, we can see
 579 some fluctuation around a steady state. The bottom part
 580 of the figure are density plots of trajectories of pedestri-
 581 ans during the control-free simulations for the parameter

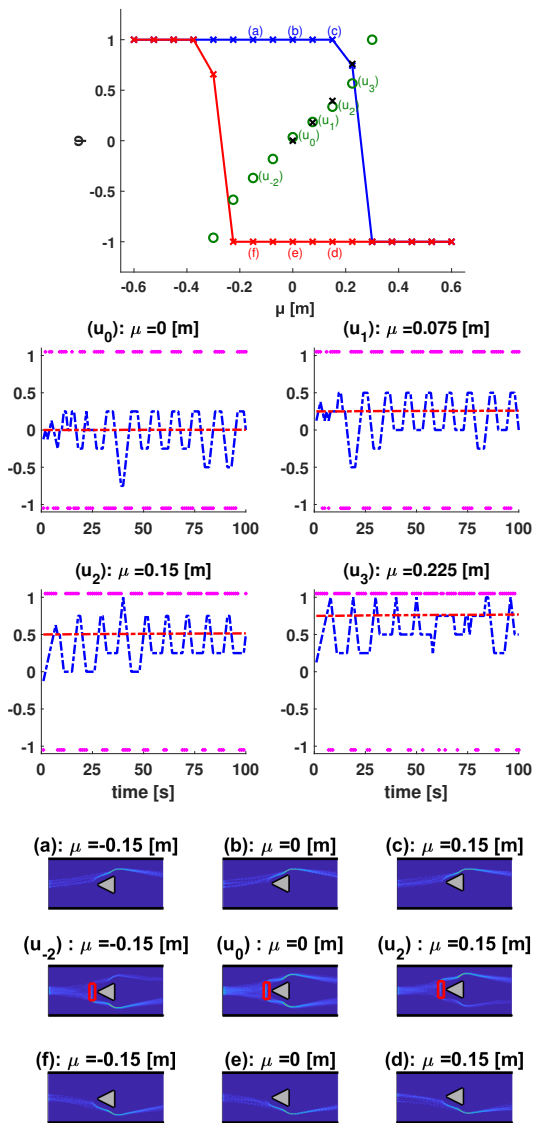


FIG. 5. Numerical simulations of control of pedestrian flows. Top: flux difference φ is plotted over the obstacle position. Stabilised target states (green circles) for different positions of the obstacle reveal the unstable branch. For comparison, experimental results are shown by black crosses (see Fig. 4). Flux difference without control for up- (blue) and downswep (red) of the parameter (compare with Fig. 2). Middle: the measured control flux difference φ_t as a function of time (blue: actual flux difference), the state of the controller y_t which estimates the target state (red), and the time trace of the pedestrian count passing by the obstacle, p_t (purple circles). Bottom: density plots of pedestrians for different positions of the obstacle (grey triangle) without control - parameter upswep (a-c) and parameter downswep (d-f) - and density plots with control (u_{-2} , u_0 , u_2). The red rectangle in front of the obstacle indicates the control area, only pedestrians in this area are affected by the control input.

582 upswep (a-c) and downswep (f-d) and density plots during
583 the control procedure (u_{-2} , u_0 , u_2). Comparing the

584 density plots subjected to control, panels (u_{-2} , u_0 , u_2),
585 to those without control, panels (a-f), we clearly see that
586 the control strategy manages to disentangle the pedestrian
587 flow efficiently. Furthermore, if we switch off the
588 control the system returns to the stable branches, thus
589 giving again evidence that the stabilised patterns are un-
590 stable states of the system.

591 We thus have compelling evidence that the model out-
592 lined in this section is able to capture details of the ex-
593 perimental pedestrian flow even at a quantitative level.
594 It is, however, important to stress that such an accu-
595 rate model is by no means needed to analyse pedestrian
596 flows within our model-free approach. The detection of
597 suitable unstable states which can be used for a soft man-
598 agement strategy can be accomplished solely by a simple
599 control tool. The outcome of the procedure is a bifur-
600 cation analysis at a macroscopic level which is sufficient
601 to uncover the relevant dynamical features of our flow
602 experiment. Nevertheless, accurate microscopic models
603 have their virtue as they allow for prediction and for the
604 implementation of sophisticated management strategies.
605 The accuracy of such models can then still be bench-
606 marked by a model-free analysis.

V. DISCUSSION

607
608 We have proposed an experimental testbed which is ap-
609 propriate for implementing and testing soft management
610 strategies for pedestrian flows. In particular, we suc-
611 ceeded in extracting the dynamic features of the walking
612 behaviour of pedestrians without the need of a math-
613 ematical model. Above all, bifurcation scenarios were
614 detected which can be exploited to manage crowds in a
615 real world scenario. Since the outlined approach does
616 not rely on any model, the findings are robust and sta-
617 ble as with regards to imperfections and noise. In addi-
618 tion, the protocol employed here allows to validate math-
619 ematical models of social behaviour in a quantitative way.

620 In particular, our method confirms the validity of social
621 force and related models as long as crucial ingredients
622 like the lemming effect are properly accounted for. The
623 latter provides an efficient way to take into account the
624 psychology of individuals and its impact on the overall
625 pedestrian flow. Under such conditions we obtain a quite
626 remarkable quantitative agreement between experiment
627 and model, which, a posteriori confirms the advanced
628 stage of modelling of social behaviour.
629 The density constitutes a crucial quantity for the dy-
630 namics of pedestrian flows (cf. e.g. as well [59]). While
631 a value for the density can be enforced in simulations
632 and to some extent in laboratory experiments as well, its
633 value in real world pedestrian flows is often the conse-
634 quence of the dynamics of the crowd, where individuals
635 may even evaporate from the system, if not prevented
636 by hard constraints which may result in crowd disasters.
637 To use an analogy from equilibrium statistical mechanics
638 the density behaves like in a grand canonical ensemble

639 where the chemical potential is given.

640 Within our particular setup the density plays a crucial
641 role for the occurrence of the bifurcation scenario. At
642 high densities the pedestrians jam in front of the obsta-
643 cle, the dynamics changes considerably, pedestrians pass
644 on each side of the obstacle, and the bistable dynamical
645 behaviour ceases to exist. Such phenomena occur if the
646 interpersonal distance drops below one meter, i.e., below
647 the comfortable distance people prefer, or at an inflow
648 rate to the channel which is higher than two individuals
649 per second. We have tested these numbers extensively
650 in simulations and in laboratory experiments with small
651 groups of individuals. In fact, we have observed these
652 problems when we run laboratory experiments without
653 a controlled inflow since all participants may enter the
654 corridor at the same time. In our laboratory setups we
655 regulated the inflow to 0.6 persons per second.

656 At very low densities, in particular if the pedestrians do
657 not notice each other any longer, no lemming effect dom-
658 inates the motion and the hysteresis disappears as well.
659 Such features which also come with interruptions of the
660 flow appear at interpersonal distances above 10 meters.
661 We have confirmed those values by extensive simulations
662 of the setup used in our experiments and with prelim-
663 inary experimental studies with small groups of people.
664 In our laboratory experiments we have avoided these flow
665 interruptions by a controlled inflow to the corridor.

666 The hysteresis occurs for a fairly broad range of den-
667 sities with mean interpersonal distance between one and
668 ten meters. While in simulations and laboratory experi-
669 ments such a value can be achieved by controlling the
670 inflow, most surprisingly the hysteresis also shows up in
671 the field experiment where the inflow has not been mon-
672 itored at all. Here the density itself fluctuates and the
673 interpersonal distance people prefer results in moderate
674 densities which support the bistability. All aspects which
675 come with real crowds of people such as fluctuation of
676 the inflow, people deliberately ignoring the signs, families
677 forming small groups within the stream of pedestrians, or
678 asymmetries in the geometry of the corridor have not re-
679 sulted in a breakdown of the hysteresis phenomenon. In
680 particular, unlike laboratory experiments which are nor-
681 mally done by recruiting or even paying individuals, the
682 people in our field experiment were not aware what to
683 expect, and that seems to be as well a crucial factor for
684 the hysteresis phenomenon to occur. The bistability is
685 therefore a representative scenario for people leaving or
686 entering a domain freely, i.e., it is a characteristic fea-
687 ture for a crowd of pedestrians in an environment where
688 they are able to ensure the comfortable distance between
689 people, resulting in an effective average density which
690 supports the occurrence of hysteresis.

691 Because of the discrete nature of counting people and
692 given the moderate densities employed in our experi-
693 ments, the signal processing had to cope with substantial
694 finite size effects, so that our set up cannot be captured
695 by a continuum limit for the pedestrian flow. Such a
696 challenge has impact on the setup of the control loop

697 as the signal used to adjust the sign is initially discrete.
698 Smoothing the signal by a simple low pass filter turned
699 out to be sufficient so that standard time continuous lin-
700 ear control theory could be applied.

701 Careful considerations are required to set up controlled
702 experiments successfully. Artificial boundary conditions
703 have the potential to destroy the dynamical features of
704 realistic pedestrian flows. In that respect any kind of pe-
705 riodic boundary conditions or repeated use of individuals
706 have to be taken with a pinch of salt as the memory of in-
707 dividuals may induce novel dynamical properties which
708 are otherwise absent. Hence, the two types of experi-
709 ments we have conducted were important, the laboratory
710 type experiment at the Ulmencampus (see Fig. 2) and the
711 real-world application at the port of Warnemünde (see
712 Fig. 3). In the former case clear signage and instruc-
713 tions to the participants and a constant inflow avoiding
714 disruption of the flow have been crucial. Nevertheless,
715 the qualitative dynamics of the flow is robust as proven
716 by the comparison with the crowd in Warnemünde port
717 where no particular instructions were given. However,
718 in both cases it has turned out to be necessary to pre-
719 vent a disruption of the flow as otherwise the dynamical
720 structures would have been erased from the system. Our
721 Ulmencampus experiment succeeded as a testbed for em-
722 ulating the behaviour of real world cohorts using a lab-
723 oratory set-up with less than 1000 participants. Within
724 our setup we used a low technology approach as with re-
725 gards to data recording and processing. Of course more
726 sophisticated data recording and data processing tools
727 like movement detection via video tracking could be used
728 as well. However, our studies demonstrate that such ad-
729 vanced tools may not be required in general.

730 The approach we have used can be viewed as a particu-
731 lar instalment of control-based continuation for complex
732 systems, where one tracks unstable, unobservable states
733 in dependence of system parameters. Such features are
734 crucial to understand the dynamical properties. There-
735 fore our approach can be viewed as a particular variant
736 of a spectroscopic tool. The unobservable dynamical fea-
737 tures are the major lever for control with minimal impact,
738 crowd management and soft management strategies. In
739 return, whenever a soft strategy is successfully applied,
740 as for instance in dynamical speed limits [41, 42], it is
741 worth to uncover the underlying dynamical signature us-
742 ing a model-free approach. Furthermore, unstable states
743 provide an important skeleton for any dynamical system
744 and any mathematical model has to reproduce such fea-
745 tures. In that respect our model-free and data based
746 approach can be used as well for benchmarking the ac-
747 curacy of a dynamical model.

748 Crowd management is one of the key issues with
749 huge impact on people's security and well-being as
750 vividly illustrated by the recent need to implement
751 effective social distancing measures to prevent diseases
752 from spreading [9–11]. Understanding the dynamical
753 aspects of large groups of pedestrians is at the heart of
754 implementing control measures and designing related

755 policies successfully. Our model-free approach can help 771
 756 to provide data and structures for soft management of
 757 people, e.g., understanding the effectiveness of signing
 758 systems, and underpinning the results with dynamical
 759 features of the actual pedestrian flow. For instance,
 760 it is tempting to extend our approach to evacuation
 761 scenarios. While the lemming effect has a negative
 762 impact on the time needed to evacuate a room, it looks
 763 promising to use a combination of the existing knowledge
 764 based on mathematical models and a novel data based
 765 model-free approach to find minimal invasive strategies
 766 for improving critical evacuation times of rooms and
 767 general infrastructure. We think our showcase may serve
 768 as a paradigm for future research in quantitative social
 769 science.

ACKNOWLEDGMENTS

772 The authors are greatly indebted to Ralf Ludwig from
 773 the Ulmencampus of the University of Rostock, Oliver
 774 Schubert from F.C. Hansa Rostock and to the Rostock
 775 Port authorities, in particular to Jens Käkenmeister and
 776 his colleagues for supporting the experiments at their
 777 facilities. We are thankful to members of the Insti-
 778 tute of Mathematics and other volunteers who helped
 779 us conducting various experiments. J.S. thanks the DFG
 780 for support through the Collaborative Research Center
 781 CRC 1270 (Deutsche Forschungsgemeinschaft, Grant/
 782 Award Number: SFB 1270/2-299150580). W.J. is grate-
 783 ful to EPSRC for financial support through grant no.
 784 EP/R012008/1.

-
- 785 [1] S. P. Taylor, *The Hillsborough Stadium Disaster: 15* 827
 786 *April 1989: Inquiry by the Rt Hon Lord Justice Taylor:* 828
 787 *Interim Report: Presented to Parliament by the Secre-* 829
 788 *tary of State for the Home Department by Command of* 830
 789 *Her Majesty August 1989* (HM Stationery Office, 1989). 831
 790 [2] M. Pretorius, S. Gwynne, and E. R. Galea, Large crowd 832
 791 modelling: an analysis of the duisburg love parade disaster, 833
 792 *Fire and Materials* **39**, 301 (2015). 834
 793 [3] K. Moodie, The king’s cross fire: damage assessment and 835
 794 overview of the technical investigation, *Fire Safety Jour-* 836
 795 *nal* **18**, 13 (1992). 837
 796 [4] D. Helbing, A. Johansson, and H. Z. Al-Abideen, Dy- 838
 797 namics of crowd disasters: An empirical study, *Physical* 839
 798 *Review E* **75**, 046109 (2007). 840
 799 [5] D. Helbing and A. Johansson, *Pedestrian, crowd and* 841
 800 *evacuation dynamics* (Springer, 2009). 842
 801 [6] A. Schadschneider, W. Klingsch, H. Klüpfel, T. Kretz, 843
 802 C. Rogsch, and A. Seyfried, Evacuation dynamics: Em- 844
 803 pirical results, modeling and applications, *Encyclopedia* 845
 804 *of Complexity and Systems Science* , 3142 (2009). 846
 805 [7] S. Sarkar, Qualitative evaluation of comfort needs in ur- 847
 806 ban walkways in major activity centers, *Transportation* 848
 807 *Quarterly* **57**, 39 (2003). 849
 808 [8] P. Dallard, T. Fitzpatrick, A. Flint, A. Low, R. R. Smith, 850
 809 M. Willford, and M. Roche, London millennium bridge: 851
 810 pedestrian-induced lateral vibration, *Journal of Bridge* 852
 811 *Engineering* **6**, 412 (2001). 853
 812 [9] P. Block, M. Hoffman, I. J. Raabe, J. B. Dowd, C. Ra- 854
 813 hal, R. Kashyap, and M. C. Mills, Social network-based 855
 814 distancing strategies to flatten the covid-19 curve in a 856
 815 post-lockdown world, *Nature Human Behaviour* **4**, 588 857
 816 (2020). 858
 817 [10] E. Gibney, Whose coronavirus strategy worked best? 859
 818 scientists hunt most effective policies, *Nature* **581**, 15 860
 819 (2020). 861
 820 [11] N. Jones, How coronavirus lockdowns stopped flu in its 862
 821 tracks. nature news. 21 may 2020, URL: [https://www.](https://www.nature.com/articles/d41586-020-01538.8) 863
 822 [nature.com/articles/d41586-020-01538.8](https://www.nature.com/articles/d41586-020-01538.8). 864
 823 [12] E. R. Galea, A general approach to validating evacuation 865
 824 models with an application to exodus, *Journal of Fire* 866
 825 *Sciences* **16**, 414 (1998). 867
 826 [13] D. C. Duives, W. Daamen, and S. P. Hoogendoorn, State- 868
 of-the-art crowd motion simulation models, *Transporta-*
tion Research Part C: Emerging Technologies **37**, 193
 (2013).
 [14] D. Chowdhury, L. Santen, and A. Schadschneider, Statis-
 tical physics of vehicular traffic and some related systems,
Physics Reports **329**, 199 (2000).
 [15] D. Helbing, I. Farkas, and T. Vicsek, Simulating dynam-
 ical features of escape panic, *Nature* **407**, 487 (2000).
 [16] D. R. Parisi, R. Cruz Hidalgo, and I. Zuriguel, Active
 particles with desired orientation flowing through a bot-
 tleneck, *Scientific Reports* **8**, 9133 (2018).
 [17] A. Kirchner, H. Klüpfel, K. Nishinari, A. Schadschnei-
 der, and M. Schreckenberg, Simulation of competitive
 egress behavior: comparison with aircraft evacuation
 data, *Physica A: Statistical Mechanics and its Applica-*
tions **324**, 689 (2003).
 [18] M. Campanella, S. Hoogendoorn, and W. Daamen, Ef-
 fects of heterogeneity on self-organized pedestrian flows,
Transportation Research Record: Journal of the Trans-
portation Research Board , 148 (2009).
 [19] A. Beard, R. Carvel, *et al.*, *The handbook of tunnel fire*
safety (Thomas Telford London, 2005).
 [20] M. Kobes, I. Helsloot, B. De Vries, and J. G. Post, Build-
 ing safety and human behaviour in fire: A literature re-
 view, *Fire Safety Journal* **45**, 1 (2010).
 [21] B. Steffen and A. Seyfried, Methods for measuring pedes-
 trian density, flow, speed and direction with minimal
 scatter, *Physica A: Statistical Mechanics and its Applica-*
tions **389**, 1902 (2010).
 [22] S. Heliövaara, J.-M. Kuusinen, T. Rinne, T. Korhonen,
 and H. Ehtamo, Pedestrian behavior and exit selection
 in evacuation of a corridor—an experimental study, *Safety*
Science **50**, 221 (2012).
 [23] A. Nicolas, M. Kuperman, S. Ibañez, S. Bouzat, and
 C. Appert-Rolland, Mechanical response of dense pedes-
 trian crowds to the crossing of intruders, *Scientific Re-*
ports **9**, 105 (2019).
 [24] A. Garcimartín, J. Pastor, C. Martín-Gómez, D. Parisi,
 and I. Zuriguel, Pedestrian collective motion in competi-
 tive room evacuation, *Scientific reports* **7**, 10792 (2017).
 [25] D. Helbing, L. Buzna, A. Johansson, and T. Werner,
 Self-organized pedestrian crowd dynamics: Experiments,

- 869 simulations, and design solutions, *Transportation Science* 933
870 **39**, 1 (2005). 934
- 871 [26] M. Boltes and A. Seyfried, Collecting pedestrian trajec- 935
872 tories, *Neurocomputing* **100**, 127 (2013). 936
- 873 [27] A. Corbetta, L. Bruno, A. Muntean, and F. Toschi, High 937
874 statistics measurements of pedestrian dynamics, *Trans- 938*
875 portation Research Procedia **2**, 96 (2014). 939
- 876 [28] Arunabha Banerjee, Akhilesh Kumar Maurya and Gre- 940
877 gor Lämmel, A review of pedestrian flow characteristics 941
878 and level of service over different pedestrian facilities, 942
879 *Coll. Dyn.* **3**, 1 (2018). 943
- 880 [29] Lakshmi Devi Vanumu, K. Ramachandra Rao and Gee- 944
881 tam Tiwari, Fundamental diagrams of pedestrian flow 945
882 characteristics: A review, *Eur. Transp. Res. Rev.* **9**, 49 946
883 (2017). 947
- 884 [30] S. P. Hoogendoorn and W. Daamen, Pedestrian behavior 948
885 at bottlenecks, *Transp. Sci.* **39**, 147 (2005). 949
- 886 [31] A. Jelic, C. Appert-Rolland, S. Lemerrier and J. Pettre, 950
887 Properties of pedestrians walking in line: Fundamental 951
888 diagrams, *Phys. Rev. E* **85**, 036111 (2012). 952
- 889 [32] J. Zhang and A. Seyfried, Empirical Characteristics of 953
890 Different Types of Pedestrian Streams, *Proc. Eng.* **62**, 954
891 655 (2013). 955
- 892 [33] M. Moussaid, E.G. Guilloit, M. Moreau, J. Fehrenbach, 956
893 O. Chabiron, S. Lemerrier, J. Pettré, C. Appert-Rolland, 957
894 P. Degond and G. Theraulaz, Traffic Instabilities in Self- 958
895 Organized Pedestrian Crowds, *PLoS Compu. Biol.* **8** 959
896 e1002442 (2012). 960
- 897 [34] A. Corbetta, J.A. Meeusen, C. Lee, R. Benzi and F. 961
898 Toschi, Physics-based modeling and data representation 962
899 of pairwise interactions among pedestrians, *Phys. Rev. E* 963
900 **98**, 062310 (2018). 964
- 901 [35] A. Schadschneider and A. Seyfried, Empirical results for 965
902 pedestrian dynamics and their implications for modeling, 966
903 *Netw. and Hetero. Media* **6**, 545 (2011). 967
- 904 [36] P. Geoerg, J. Schumann, M. Boltes and M. Kinateder, 968
905 How people with disabilities influence crowd dynamics of 969
906 pedestrian movement through bottlenecks, *Sci. Rep.* **12**, 970
907 14273 (2022). 971
- 908 [37] C. Harrison, N. Kukadia, P. Stoneman and G. Dyer, Pilot 972
909 for Standing on Both Sides of Escalators, in *Proceedings 973*
910 *of the 6th Symposium on Lift and Escalator Technologies*, 974
911 (Northampton 2016). 975
- 912 [38] W. Challenger, W. Clegg, and A. Robinson, Understand- 976
913 ing crowd behaviours: Guidance and lessons identified, 977
914 UK Cabinet Office , 11 (2009). 978
- 915 [39] S. A. Richmond, A. R. Willan, L. Rothman, A. Cam- 979
916 den, R. Buliung, C. Macarthur, and A. Howard, The 980
917 impact of pedestrian countdown signals on pedestrian- 981
918 motor vehicle collisions: a reanalysis of data from a quasi- 982
919 experimental study, *Injury Prevention* **20**, 155 (2014) 983
920 . 984
- 921 [40] I. Panagiotopoulos, J. Starke, and W. Just; Pedestrian 985
922 Flow Experiment at the Ulmencampus of the Univer- 986
923 sity of Rostock. See Supplemental Material at [URL will 987
924 be inserted by publisher] for Blurred Video Sequence of 988
925 Transition in Route Choice (2022). 989
- 926 [41] R. L. Bertini, S. Boice, and K. Bogenberger, Dynam- 990
927 ics of variable speed limit system surrounding bottleneck 991
928 on german autobahn, *Transportation Research Record* 992
929 **1978**, 149 (2006). 993
- 930 [42] B. Khondaker and L. Kattan, Variable speed limit: A 994
931 microscopic analysis in a connected vehicle environment, 995
932 *Transportation Research Part C: Emerging Technologies* 996
58, 146 (2015).
- [43] C. Fuhs and P. Brinckerhoff, *Synthesis of Active Traf- 934*
fic Management Experiences in Europe and the United 935
States, Tech. Rep. (United States. Federal Highway Ad- 936
ministration, 2010). 937
- [44] T. Shinbrot, C. Grebogi, J. A. Yorke, and E. Ott, Using 938
small perturbations to control chaos, *Nature* **363**, 411 939
(1993). 940
- [45] C. I. Siettos, I. G. Kevrekidis, and D. Maroudas, Coarse 941
bifurcation diagrams via microscopic simulators: a state- 942
feedback control-based approach, *International Journal 943*
of Bifurcation and Chaos **14**, 207 (2004). 944
- [46] S. Misra, H. Dankowicz, and M. R. Paul, Event-driven 945
feedback tracking and control of tapping-mode atomic 946
force microscopy, *Proceedings of the Royal Society A: 947*
Mathematical, Physical and Engineering Sciences **464**, 948
2113 (2008). 949
- [47] J. Sieber and B. Krauskopf, Control based bifurcation 950
analysis for experiments, *Nonlinear Dynamics* **51**, 365 951
(2008). 952
- [48] D. A. Barton and J. Sieber, Systematic experimental ex- 953
ploration of bifurcations with noninvasive control, *Phys- 954*
ical Review E **87**, 052916 (2013). 955
- [49] J. Sieber, A. Gonzalez-Buelga, S. Neild, D. Wagg, and 956
B. Krauskopf, Experimental continuation of periodic or- 957
bits through a fold, *Physical Review Letters* **100**, 244101 958
(2008). 959
- [50] E. Bureau, F. Schilder, I. F. Santos, J. J. Thomsen, and 960
J. Starke, Experimental bifurcation analysis of an impact 961
oscillator—tuning a non-invasive control scheme, *Journal 962*
of Sound and Vibration **332**, 5883 (2013). 963
- [51] K. Pyragas, V. Pyragas, I. Kiss, and J. Hudson, Stabi- 964
lizing and tracking unknown steady states of dynamical 965
systems, *Physical Review Letters* **89**, 244103 (2002). 966
- [52] I. G. Kevrekidis, C. W. Gear, J. M. Hyman, P. 967
G. Kevrekidis, O. Runborg, and C. Theodoropoulos, 968
Equation-free, coarse-grained multiscale computation: 969
Enabling microscopic simulators to perform system-level 970
analysis, *Commun. Math. Sci.* **1**, 715 (2003). 971
- [53] N. Bellomo and C. Dogbe, On the modeling of traffic and 972
crowds: A survey of models, speculations, and perspec- 973
tives, *SIAM review* **53**, 409 (2011). 974
- [54] E. Papadimitriou, G. Yannis, and J. Golias, A critical 975
assessment of pedestrian behaviour models, *Transporta- 976*
tion Research Part F: Traffic Psychology and Behaviour 977
12, 242 (2009). 978
- [55] A. L. Bazzan and F. Klügl, *Multi-agent systems for traf- 979*
fic and transportation engineering (Information Science 980
Reference, 2009). 981
- [56] D. Helbing and P. Molnar, Social force model for pedes- 982
trian dynamics, *Physical Review E* **51**, 4282 (1995). 983
- [57] J. Starke, K. B. Thomsen, A. Sørensen, C. Marschler, 984
F. Schilder, A. Dederichs, and P. Hjorth, Nonlinear ef- 985
fects in examples of crowd evacuation scenarios, in *17th 986*
International IEEE Conference on Intelligent Trans- 987
portation Systems (ITSC) (IEEE, 2014) pp. 560–565. 988
- [58] I. Panagiotopoulos, J. Starke, J. Sieber, and W. Just; 989
Continuation with Non-invasive Control Schemes: Re- 990
vealing Unstable States in a Pedestrian Evacuation Sce- 991
nario. To appear in *SIAM Journal on Applied Dynamical 992*
Systems. 993
- [59] I. Echeverría-Huarte, A. Garcimartín, R. C. Hidalgo, C. 994
Martín-Gómez, and I. Zuriguel , Estimating density lim- 995
its for walking pedestrians keeping a safe interpersonal 996

